Automated estimation of tiller number in wheat by ribbon detection

Boyle, R. D.; Corke, F. M. K.; Doonan, J. H.

Published in:
Machine Vision and Applications

DOI:
10.1007/s00138-015-0719-5

Publication date:
2016

Citation for published version (APA):
Boyle, R. D., Corke, F. M. K., & Doonan, J. H. (2016). Automated estimation of tiller number in wheat by ribbon detection. *Machine Vision and Applications*, *27*(5), 637-646. https://doi.org/10.1007/s00138-015-0719-5

Noname manuscript No.
(will be inserted by the editor)

Automated estimation of tiller number in wheat by ribbon detection

R D Boyle · F M K Corke · J H Doonan

the date of receipt and acceptance should be inserted later

Abstract The advent of high-throughput phenotyping installations signals a need for plant biology to use pattern analysis and recognition techniques, especially when analysis is done via digital images. Such installations also provide an opportunity to computer vision.

We describe one such application at the UK National Plant Phenomics Centre, in which historically measurements have been made in a labour-intensive manual manner. We develop an estimator of tiller number in growing wheat which, when exploiting per-day averaging, temporal interpolation and dynamic programming, delivers measurements of finer-grain and no less accuracy than manually, and provides observations on plant treatments hitherto difficult or impossible to obtain.

The approach developed lends itself to reuse for any similar imaging setup, and plants with tillering characteristics similar to wheat. We consider the work a useful exemplar for co-operation between biologists and computer scientists in such installations.

Keywords Small grain cereals · branching · plant development · computer vision

1 Introduction

Worldwide, there is increasing interest in applying imaging technologies to plant phenotyping [9], and a growing number of installations able to perform large scale phenotyping experiments – [1, 14, 17] are just some examples. Usually, these are based on automated greenhouses that can administer pre-programmed treatments to a number of plants, of which they likewise make regular automated measurements. These installations permit large scale experiments to be conducted over time within complex regimes, with minimal staff input. Much can be gained from the simplest of monitoring such as a photograph, but a variety of other image modalities (UV, IR, NIR, structured light), and root analysis, are also available. Measurements of benefit to biologists can then fall into a number of categories:

1. Replication/mimicry of 'simple' measurements performed manually. These include plant height and projected area (which can be used to approximate mass).
2. (which can be used to approximate mass).
3. Replication/mimicry of less easily accessible measurement, for example, atlas growth stages.
4. Measurements that may be of benefit that have not been made systematically in the past.

These developments are timely as computer vision also continues to make significant theoretical and practical progress [23]. High throughput phenotyping installations represent very fertile territory for many such algorithms. We might seek to develop measurements accessible to computer extraction that would be difficult or costly if collected manually. Such activity has been growing in popularity in recent years, for example [3, 4, 11, 19, 21, 22].

In this paper we present work in progress on one such example: tiller counting in wheat. The architecture of individual plants has profound implications for

R D Boyle · F M K Corke · J H Doonan
National Plant Phenomics Centre
IBERS, Aberystwyth University
Plas Gogerddan, SY23 3EB, U.K.
E-mail: {rob21,fic5,john.doonan}@aber.ac.uk

Fig. 1 The UK NPPC. Left, One of the robotic greenhouses; Right, Plants (here, maize) entering the imaging chambers.

productivity and reproductive success – tiller number is generally scored manually, often at harvest as an end-of-life trait but availability of automated plant phenotyping platforms holds the promise of automating this process and allowing dynamic measurements during development and in response to environmental perturbation. We consider this application to fall between (2) and (3) above. It is probable that the approach we present would generalise to related cereals such as rice and millet.

2 Background

2.1 Tillering in wheat

Crop domestication is often associated with architectural modification. One of the most extreme examples of domestication-associated modification has occurred during domestication of maize where the modern crop plant is typically comprised of a single stem. The wild ancestor, teosinte, forms numerous basal branches (referred to as tillers in the grass family) and modification of a single gene (Teosinte branched 1) largely suppresses this process [16] so that the cultivated maize plant generally has a single tiller and no tillers. This mechanism appears to be conserved in the grasses, including rice [5], but in other grain crops, tillering has not been so highly modified. Nevertheless, tiller number is a key agronomic trait that is thought to contribute to yield, perhaps through canopy structure and light interception [13, 20].

The number of tillers in wheat and related crops is determined early in the life cycle [2, 15] and is influenced by genotype, water availability and nutrition [18]. For example, the duration of tillering is influenced by the ratio of red/far red light [6, 7]. Shading regulates the extent of tillering in maize and other grasses through the grassy tillers1 gene [24]. Overproduction of tillers can be detrimental to yield as infertile tillers may compete with fertile ones [10], and to quality as a crowded canopy can be more susceptible to disease and pests [12].

Objectively quantifying variation in tiller number, or many other architectural traits, with a view to understanding plant performance or to exploiting that variation in breeding therefore remains a challenge. Manual counting of any but small data sets is time-consuming and for productive plants errors of ± 2 tillers may easily be experienced. Counting is often made at harvest as an end-of-life trait. The potential for adequate (in the sense of no-worse) automatic estimates, coupled with day-to-day measurement, is therefore very attractive.

Automated measurement of tiller number should facilitate the dynamic dissection of this key agronomic trait but presents a number of challenges, notably visual occlusion. Good quality measurements of the tiller number statistic are not easy to obtain, especially in quantity, and no generally accepted non-manual procedures are known for monitoring tiller number during the life of the plant.

2.2 Imaging environment

The UK National Phenomics Centre (NPPC) has recently been established at the university of Aberystwyth and exists to conduct large scale phenomics experiments. The full facility is described elsewhere [17]; it affords a variety of imaging modalities and opportunities for controlled environments and treatments. Here, it is sufficient to appreciate that up to 850 plants can be imaged in various modalities daily under specified conditions. Imaging can include rotated and birds-eye view pictures of each plant – see Figure 1.

Fig. 2 Three images of the same plant, rotated $0°, 45°, 90°$. This plant was grown under 75% field capacity and the images acquired toward the end of the experiment (March 28^{th} 2014).

2.3 Ribbon identification

In the images we see (for example, Figure 2), inspection suggests that tillers appear as ribbons that are vertical or near vertical, and usually of breadth in the range 6-10 pixels. This information alone is insufficient to distinguish them, as the leaves often have similar properties; nevertheless, our first step was to attempt to isolate all such features. The problem has similarities to the location of other ribbon like structures (for example, blood vessels and airways) in medical images. This is a long-studied problem in which the Frangi 'vesselness' filter [8] has found much favour. The filter takes a grey level input and at each pixel considers the evidence for it being the mid-point of a ribbon (in 3D, a cylinder). It returns a score of such evidence, along with a matrix recording the most responsive ribbon width and a second matrix recording direction. This is done by considering the eigenvalues of the Hessian matrix at that pixel over the scale range defined: their relative size and signs betray the geometry local to the pixel at the chosen scale. 'Scale' determines the σ (standard deviation) of a Gaussian convolution: the filter actually seeks ribbons of width 2σ. The filter determines the scale (and direction) of the maximal ribbon-like response. Figure 6 below illustrates this for a small image.

3 Tiller number estimation in wheat

In this study a large number of 2D images were taken of 60 plants over an 8 week period. Analysing the basal regions of these images and identifying tiller-like structures provides a 12-dimensional feature which we use to estimate the number of tillers present: note this is an indirect procedure inasmuch as we do not identify tillers explicitly, but rather make an estimate of their number. Limited manually acquired ground truth then permits a regression estimate from this feature to give the number of tillers evident. The estimate can be improved by combining (cheaply obtained) multiple views, after which the time series of noisy estimates may be further improved by dynamic programming to determine the most likely development over the interval.

Spring wheat (Paragon) was sown 2 seeds/pot in 8cm square pots of Levington F2 compost and then singled and transplanted to weighed 2.5L pots of F2+40% grit sand. Pots were filled to a uniform weight to allow target watering to be applied at selected water regimes. Plants were transferred to an automated conveyor system (Lemnatec, Aachen, Germany) for controlled watering and imaging. Plants were grown at 18^oC (± 5) day, 15^oC (± 3) night with a 14 hour photoperiod. Sixty plants in total were split over 5 watering regimes (15%, 30%, 45%, 60% and 75% of field capacity were calculated from dry matter and field capacity measurements on the same growth medium); these regimes were chosen to produce plants of very different stature. Manual counts of tillers (unambiguously present when $> 2cm$ long, and just becoming evident in images) were made throughout the phase of tiller production (22-70 days after sowing [DAS]) with destructive harvesting of a subset of plants between 49-70 DAS. Destructive harvesting scored the plants for fertile tiller number, height, fresh and dry weight and harvest index.

The NPPC facility permits imaging with a variety of modalities at many orientations: in this experiment, only RGB (visible spectrum) was used, with 3 side view images per day, with the plant rotated through positions 0^o, 45^o and 90^o. RGB images of 2456x2054

Fig. 3 Pairs of images of three example plants, recorded at early development and after tillering is complete. At left, 1 tiller at maturity; at centre five; at right, 10 tillers.

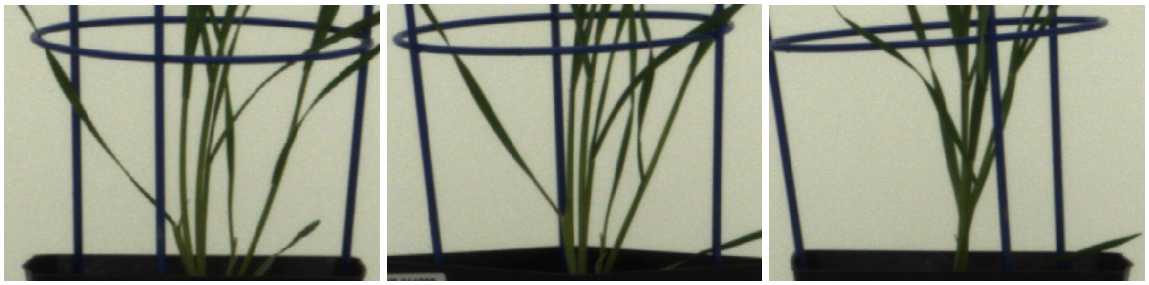

Fig. 4 Three view of a particular plant 32 days after sowing – various ribbon like structures are evident, but the rightmost (90°) image self-occludes a great deal. Ground truth counting reveals 5 tillers on this plant on this day.

pixel resolution were collected with imaging occurring on most days, resulting in a final number of approximately 7500 images. A combination of manufacturer and in-house software provide immediate simple measurements such as plant height and 2D-projected bulk, which is a good index to biomass. Blue is an artificial colour in plant scenes and can be readily removed from the images by segmentation, and is therefore is used for the carriage, the plant supports and registration points in the scene. Figure 3 illustrates three plants before and after tillers have developed – the most populous seen during the experiment had more than 16 tillers, being much more congested than the rightmost here. Figure 4 shows a plant with 5 tillers from the three views we take – the ambiguity and problems of occlusion are clear. Figure 5 (left) is a close-up of part of the leftmost plant in Figure 2 in which the tillers are evident; Figure 5 (right) shows the actual inspection window used.

Determining such a sub-image automatically is trivial given knowledge of the scene geometry, and pot and frame characteristics. It was assumed that any tillers would be evident directly above the pot and beneath the circular ring of blue frame, and hence an image section of dimension 200×300 that approximated this region was selected. Blue artefacts were suppressed and resulting features converted to grey, as illustrated in Figure 5. However, it is clear that this image alone is inadequate for tiller-counting: there is considerable occlusion, and interference from leaves that very often have the same or very similar local appearance as a tiller. Over time the colour patterns of the plant move from green to yellow as senescence develops, adding to the complexity.

Our suggested algorithm makes an estimate of the tillers present in an image such as Figure 5. Given such an estimate it was possible to improve on it in two ways:

- Since there were three images taken on each day $(0^o, 45^o, 90^o)$, these estimates were averaged over the per-day estimates.
- Over the period of the experiment the plants were growing and an assumption was made that there would not be a decline in main tiller count. Thus it is possible to take a series of estimates and seek

Fig. 5 Left: A typical basal region of a wheat plant used for analysis of tiller number. This image illustrates clearly the congestion at the plant base where near-vertical artefacts may be tillers or leaves. As the plant matures, some leaves will fall downward compounding the confusion. Right: The actual inspection window used; blue artefacts (the support frame) have been suppressed and the image converted to grey.

a 'best possible' adjustment to make it monotonic increasing.

To determine the preliminary estimates, recall that the Frangi filter delivers a 'strength' estimate for evidence at various ribbon widths. It should be clear that in a ribbon of width 2σ, while the central skeleton pixels will give a high response at scale σ, neighbouring pixels will give lesser, but positive, responses at neighbouring scales. These lesser, 'ghost' responses can be suppressed by performing directional non-maximal suppression [23] – this may be seen at the right of Figure 6. For each positive response in this skeleton the filter delivers an associated strength, scale and direction. It is clear that the derived skeletons are imperfect.

Tillers by their nature are close to vertical, and so it is reasonable to select some angle θ and erase evidence at pixels which deviate from the vertical by an angle exceeding this threshold. This results in an image in which non-zero entries record locally maximal evidence for a near-vertical ribbon, whose direction and breadth are recorded in the companion matrices output by the filter.

A scale range of $\sigma = 0.5, 1.0 \ldots 6.0$ was used to be sure to cover the range of tiller breadths. For each value of σ in this range, the sum of evidence for (near-)vertical ribbons of that width was computed. This delivers 12 scalars which can each be considered an estimate of total evidence for tillers of the relevant width (corrupted by noise). These scalars are taken as a 12-dimensional feature vector describing the image – this simple feature is used to estimate the number of tillers present. This is done by deriving a mapping from this feature space to known tiller count in a set of images of plants for which manual observations have been made.

In normal circumstances, images were available for each day and so the mean of the estimates derived from each view was used as a best-estimate of tiller count for each plant on a given day. This resulted for each plant in a time series of estimates, which at times had gaps of 1 or more days if the imaging was not complete. It is reasonable to assume that the number of tillers was monotonic increasing, and the last stage therefore took the time series and perturbed it via dynamic programming to derive a 'best possible' monotonic fit to the estimated data.

Implementation specifics of the algorithm are given in the next section – at a high level it may be summarised as:

1. For an input RGB image I, segment, remove blue artefacts, and convert to grey-scale the area directly above the pot rim, giving image J.
2. Run a Frangi filter with $\sigma = 0.5, \ldots 6$, giving strength image S_J, scale image W_J and direction image D_J.
3. Perform a directional non-maximal suppression of S_J with respect to D_J.
4. Erase to zero elements of S_J for which D_J is far from vertical.
5. Set
$$f_i = \sum_{\mathbf{p} \in (W_J = i)} S_J(\mathbf{p})$$
and
$$\mathbf{f}(I) = \mathbf{f}(J) = (f_{0.5}, f_{1.0}, \ldots, f_6)$$
6. From a ground-truthed training set T, determine a best fit tiller-counting function $t(\mathbf{f}(I))$. (This is outlined in Section 4).
7. For a given plant, consider the days $d_1, \ldots, d_T$ on which it has been imaged, and from which angles $\theta = 0^0, 45^o, 90^o$ (circumstances mean that the day series may not be consecutive, and very

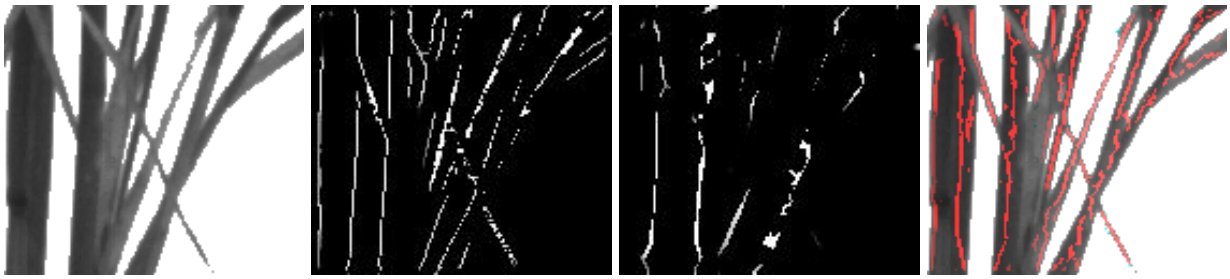

Fig. 6 Left: A part of the image at right of Figure 5, then representations of the Frangi filter response for scales $\sigma = 1.5, 4.5$. At right, in red, the non-maximally suppressed filter output overlaid on the original, giving a skeletal representation of the input.

occasionally particular angles are mis-processed by the system. This is a rare event – less than 1%.). This gives an image set $I_{d,\theta}$, and associated tiller estimates $t_{d,\theta} = t(\mathbf{f}(I_{d,\theta}))$.

8. Set $t_d = mean_\theta(t_{d,\theta})$.
9. Consider the sequence $t_{d_1}, \ldots, t_{d_T}$. Use dynamic programming optimally to convert this to a monotonic increasing sequence $\hat{t}_{d_1}, \ldots, \hat{t}_{d_T}$, where $\hat{t}_{d_i} \leq \hat{t}_{d_{i+1}}$, which has an estimate for all days in the range $[d_1, d_T]$. (This is outlined in Section 4).

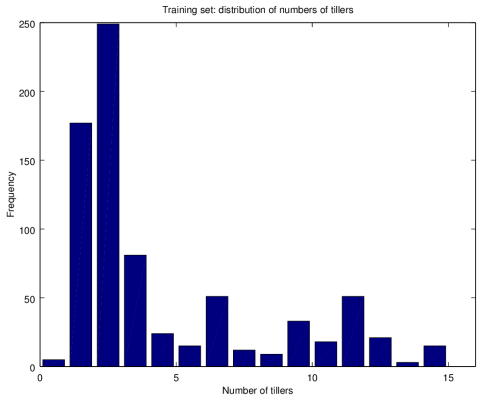

Fig. 7 The distribution of tiller numbers in the training set, between 22 and 70 days after sowing. It is clear that the bulk of these come from less-developed plants, which may be a weakness in results.

4 Implementation and results

This algorithm was applied to the 7500 images of wheat. The Frangi algorithm was deployed, and the 'verticalness' threshold was set to $\frac{\pi}{4}$ to catch any response closer then vertical than horizontal. Arguably this could be stricter and may have to be adjusted for other species or growth conditions.

The training set T was collected during the experiment via manual counting on selected days: approximately 12 plants were measured at intervals of 4-5 days whilst the plants were located on the conveyor. These measurements may well be prone to error, especially in higher numbers of tillers. Further, partial harvests were taken on 4 occasions: 2 replicates of each treatment were taken for destructive measurement. This allowed more accurate measurement. In all, approximately 750 images were labelled with reliable tiller numbers. The distribution of the manually acquired tiller count information (see Figure 7) is skewed to lower numbers since all plants passed through this phase but some (on the more severe drought regime) progressed no further.

There are many ways of moving from the 12D descriptor to tiller number: certainly a simple correlation with a 'weight of evidence' measure ($\sum_i f_i(I)$) would be one, and this does indeed give usable results. A simple linear function from 12-space to scalar was chosen to fit, in a least-squared error sense, which performed better on the data:

$$t(\mathbf{f}(I)) = b_0 + \sum_{i=0.5}^{6} b_i f_i$$

The actual size of tillers is then exploited in the scale components. An informal inspection of each of the 12 features suggests that correlation of an individual feature with tiller number exceeds 0.6 for $\sigma \geq 2$.

We have applied this very elementary estimator to our data: on a 'leave one out' basis (omitting test data from the training set) we see a mean square error (per plant) in tiller number in the region of 1.5. There is high variance in this observation – some 25% of estimates exceed 2 and are of questionable value.

Averaging estimates over a day's data was straightforward and leads to an immediate improvement, with the mean square error per plant (measured similarly) reducing to 1.05. Usually there were three estimates per day and the variance between them

rarely exceeded 1, although there was a fair incidence of rogue images that cause significant variations. Using a median instead of mean produces indistinguishable results.

Given the known behaviour of plants, it is possible to use these per-day estimates as a basis to estimate a time series. Plants have never been observed to develop 3 new tillers in a day, and 2 is very unusual, so t_{i+1}, the estimate on day $i+1$, will be at least t_i, but will not exceed it by more than 2. Thus we can take the series of estimates $t_{d_1}, \ldots, t_{d_T}$, interpolate it (linearly) to give estimates on all days, then apply dynamic programming with the assumptions

1. $t_{d_1} = 1$.
2. $t_{i+1} - t_i \leq 2$: the costs encourage this difference to be 0.

These are clearly strict assumptions, but entirely reasonable for the application.

Figure 8 illustrates just two applications of this process on individual plants (ground truth as blue points, estimates as red; the blue line shows the final best estimate of the dynamic programming) – in each case, the estimates are made from a model derived *without* using the particular plant being examined. Where the ground truth for a particular plant was known, results were rarely worse than that shown in the left figure while the right Figure shows an example of a very good fit. Note that the algorithm assumes that tiller number for an individual plant is integral. The root-MSE with ground truth (which itself may well not be wholly reliable) for all data as a result of applying this algorithm was marginally more than 1.1, suggesting that the final estimate was rarely more than 2 away from truth. It is intriguing that this error is slightly worse than that of the pre-DP estimates – on examination, it is heavily skewed by evidence from 3 plants where the ground truth seems suspect[1]. Neglecting these suspect outliers, the error reduces to 1.02.

Clearly, results for individual plants would have error bars of at least ± 1, but intra-class plant variation was already known to be greater than this. The manual procedure was therefore mimicked by averaging over all replicates for each treatment. Figure 9 illustrates this, with indicators of ground truth overlaid, where it is known. The variability of this illustrates intra-class variation. The overall trends are clear for the progressively harsher treatments and indicates that the discriminatory power of this approach is at least similar to manually acquired data sets. It is these per-treatment trends that such experiments are conducted to determine, and these results vindicate our approach. Furthermore, the rate of development under the different regimes is also clear – this is a datum that would not normally be recorded by manual observation since collecting it during the growth phase is very labour-intensive.

Without expensive complete ground truthing, it is difficult to know exactly how robust these results are. The plot overlays ground truth where the latter is known, which suggests that in the majority these lines are plausible. Treatment 3 (plotted in blue) shows the greatest deviation from ground truth and is plotted in further detail in the right of the Figure. The intra-class variation seen was well within the bounds of expectation but the model found the later observations hard to accommodate. This may be due to the oversimplification of the linear estimator but may equally demonstrate imprecise manual ground truth of densely tillered plants.

5 Conclusions and further work

Tiller counting is of importance in monitoring development of many plants, in particular wheat. Along with many traits, it is labour intensive (and often inaccurate) to collect manually, and the advent of high throughput systems makes automated estimates of tiller number attractive. We have presented such a system which makes such estimates. In isolation, occlusion and other imaging effects mean that these are unlikely to be particularly reliable. However, when combined with averaging over multiple views and intelligent interpolation over time, and consideration of replicates of a treatment, they can deliver acceptable approximations to this count.

Our system has used a 'vesselness' estimator developed for medical applications, refined for this application: codes were developed in portable Matlab[2] which the authors are happy to share on request. Total processing time per plant on a standard Linux desktop is measured in seconds as the Frangi filter is very compute hungry – currently this is not an issue as the entire dataset is processed offline, but a low-level recoding of the filter is likely to provide

[1] For example, having tiller number decrease in time; this is probably attributable to different, or inexperienced observers. Especially for very well developed plants, hand counting of tillers is far from easy and may well be 1 or two out, depending on the observer's convention.

[2] MATLAB is a registered trademark of The MathWorks, Inc.

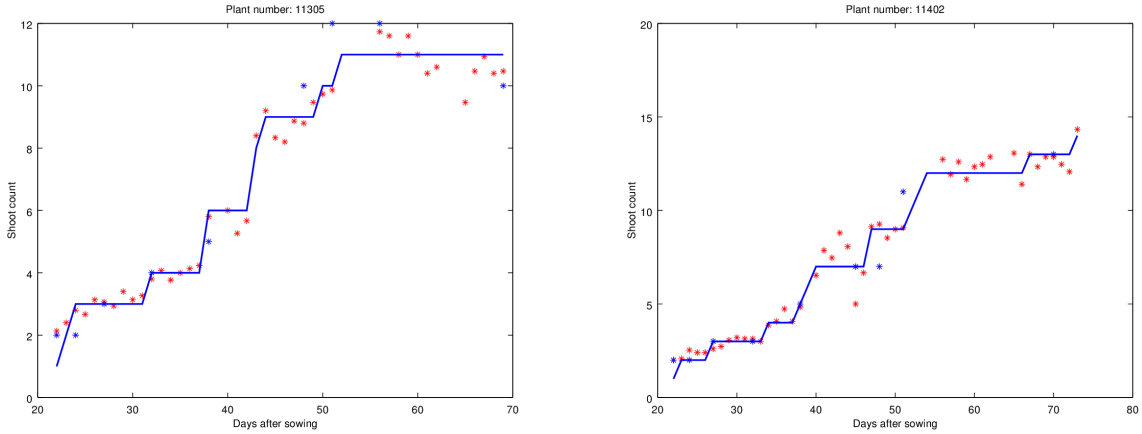

Fig. 8 Two examples of the dynamic programming procedure being applied to plant data. Red points are the estimate from the regression function $t(\mathbf{f})$ (derived without using the plant in question), blue points are known ground truth, and the line shows the dynamic programming result. (The code numbers, 11305 and 11402, refer to specific plants. 'Shoot' and 'tiller' are terms often used interchangeably.)

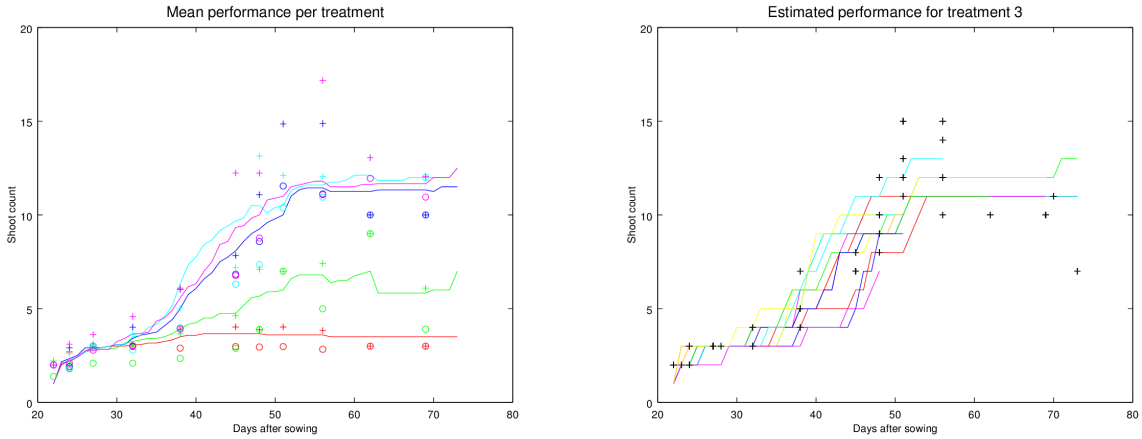

Fig. 9 Left: Averaged performance of the five different treatments. Overlaid are per-day ground truth means $\pm\sigma$ (∗,○) for days when there is more than one measurement. Right: Ground truths and estimated behaviours for treatment 3 (blue in the left graph).

an order of magnitude speedup that would obviate any issues around processing time. Overall, our results suggest a root-MSE of approximately one tiller, which is well within usable bounds and not significantly different from manual scoring. Temporal information from daily imaging then permits dynamic programming to improve day-by-day estimates significantly.

We have reported here work in progress, which can be developed in several directions to improve estimates further:

- Further wheat experiments will allow a more elaborate training set to be accumulated, in particular with more instances of 8+ tillers.
- The Frangi filter is of remarkable power and its outputs may be used in many ways: we see scope for improving the identification of putative tillers in these outputs. Any improvement in the per-image estimates of tiller number would lead to improved overall estimates.
- The regression function we use as tiller number estimator is very probably not best possible. Improving this may well be straightforward when a fuller training set (as above) is presented.
- No use has been made of colour, which could well assist in disambiguating tillers and leaves. Senescence often develops at different rates in different parts of the plant, affording a possible disambiguator.

In a high throughout automated system, measures of this kind can prove very useful in the automated study of various treatments and environments over time. Measurements made are subject to errors of

comparable magnitude to intra-class variation and human error. In principle, this approach demonstrates the feasibility of automatically extracting features from images that provide a reasonable proxy for manual tiller counts, and the method should be applicable to any crop with similar growth habit, including other small grain cereals such as rice, barley and oats. The bulk of the algorithm we present is by design elementary, and may well be amenable to significant improvement should applications require higher performance.

While this work is of direct benefit in existing experiments and high throughput installations, we see it further as an exemplar of the practicality of applying established computer vision techniques in plant breeding and biology. In cross-disciplinary work, it is critical for the computer scientist to engage properly with what the domain experimenter is trying to find out: thereafter it is possible that information automatically extractable may be of great benefit, but may not correspond directly with traditional approaches. As illustration, this application derives temporal behaviour which is very time consuming to extract manually, and can simply average over high numbers of replicates with negligible staff-time overhead. Thereby, patterns of behaviour during growth can be compared with reasonable accuracy – this has not hitherto been possible.

6 Acknowledgements

This work was supported by the Biotechnology and Biological Sciences Research Council (BBSRC grant ref numbers BB/J004405/1 and BB/J004464/1), the European Union (EPPN, an Integrating Activity, Research Infrastructure project funded by the European Union under FP7 Capacities Programme. Grant Agreement No. 284443) and the Biosciences, Environment and Agriculture Alliance (BEAA), a strategic partnership between Aberystwyth and Bangor universities. We are grateful to NPPC staff for technical support and constructive discussions.

References

1. 2014. Australian Plant Phenomics Facility. `http://www.plantphenomics.org.au/`.
2. Borras-Gelonch, G, G Rebetzke, R Richards, and I Romagosa. 2012. Genetic control of duration of pre-anthesis phases in wheat (triticum aestivum l.) and relationships to leaf appearance, tillering, and dry matter accumulation. *Journal of Experimental Botany* 63 (1): 69–89.
3. Boyle, R, F Corke, and C Howarth. 2015. Image-based estimation of oat panicle development using local texture patterns. *Functional Plant Biology* 42 (5): 433–443. `http://dx.doi.org/10.1071/FP14056`.
4. Campillo, C, M Garcia, C Daza, and M Prieto. 2010. Study of a non-destructive method for estimating the leaf area index in vegetable crops using digital images. *Hortscience* 45 (10): 1459–1463.
5. Choi, M, M Woo, E Koh, J Lee, T Ham, H Seo, and H Koh. 2012. Teosinte branched 1 modulates tillering in rice plants. *Plant Cell Reports* 31: 57–65.
6. Evers, J, J Vos, B Andrieu, and P Struik. 2006. Cessation of tillering in spring wheat in relation to light interception and red : far-red ratio. *Annals of Botany* 97: 649–658.
7. Evers, J, J Vos, M Chelle, B Andrieu, C Fournier, and P Struik. 2007. Simulating the effects of localized red:far-red ratio on tillering in spring wheat (triticum aestivum) using a three-dimensional virtual plant model. *New Phytologist* 176: 325–336.
8. Frangi, A, W Niessen, K Vincken, and M Viergever. 1998. Multiscale vessel enhancement filtering. In *Medical image computing and computer-assisted intervention – miccai98*, 130–137. Springer.
9. Furbank, R T, and M Tester. 2011. Phenomics technologies to relieve the phenotyping bottleneck. *Trends in Plant Science* 16 (12): 635–644.
10. Gallagher, J, and P Biscoe. 1978. A physiological analysis of cereal yield. ii: Partitioning of dry matter. *Agricultural Progress* 53.
11. Hartmann, A, T Czauderna, R Hoffmann, N Stein, and F Schreiber. 2011. HTPheno: An image analysis pipeline for high-throughput plant phenotyping. *BMC Bioinformatics* 12 (1): 148.
12. Hilton, AJ, P Jenkinson, TW Hollins, and DW Parry. 1999. Relationship between cultivar height and severity of fusarium ear blight in wheat. *Plant Pathology* 48: 202–208.
13. Home-Grown Cereals Authority. 2000. Optimum winter wheat plant production. `http://archive.hgca.com/publications/documents/cropresearch/topic36.pdf`.
14. 2014. Jülich Plant Phenotyping Centre. `http://www.fz-juelich.de/ibg/ibg-2/DE/Organisation/JPPC/JPPC_node.html`.
15. Lammer, D, X Cai, M Arterburn, J Chatelain, T

Murray, and S Jones. 2004. A single chromosome addition from thinopyrum elongatum confers a polycarpic, perennial habit to annual wheat. *Journal of Experimental Botany* 55 (403): 1715–1720.

16. Lukens, L, and J Doebley. 2001. Molecular evolution of the teosinte branched gene among maize and related grasses. *Molecular Biology and Evolution* 18: 627–638.
17. 2014. The UK National Plant Phenomics Centre. `http://www.plant-phenomics.ac.uk/en/`.
18. Oscarson, P. 2000. The strategy of the wheat plant in acclimating growth and grain production to nitrogen availability. *Journal of Experimental Botany* 51: 1921–1929.
19. Reis, M, R Morais, E Peres, C Pereira, O Contente, S Soares, A Valente, J Baptista, P Ferreira, and J Bulas Cruz. 2012. Automatic detection of bunches of grapes in natural environment from color images. *Journal of Applied Logic* 10 (4): 285–290.
20. Satorre, E, and G Slafer, eds. 1999. *Wheat: Ecology and physiology of yield determination.* The Haworth Press, New York.
21. Sirault, Xavier, Jurgen Fripp, Anthony Paproki, Jianming Guo, Peter Kuffner, Helen Daily, Xavier Li Rongxina nd Sirault, and Robert Furbank. 2013. PlantScan: a three-dimensional phenotyping platform for capturing the structural dynamic of plant development and growth. In *7th international conference on functional-structural plant models*, 75.
22. Song, Y, C Glasbey, G Horgan, G Polder, J Dieleman, and G van der Heijden. 2014. Automatic fruit recognition and counting from multiple images. *Biosystems Engineering* 118: 203–215.
23. Šonka, M, V Hlaváč, and R Boyle. 2014. *Image processing, analysis, and machine vision*, 4^{th} edn. CEngage.
24. Whipple, C, T Kebrom, A Weber, F Yang, D Hall, R Meeley, R Schmidt, J Doebley, T Brutnell, and D Jackson. 2011. Grassy tillers1 promotes apical dominance in maize and responds to shade signals in the grasses. *Proc Natl Acad Sci U S A* 108 (33): 506–512.